



ISSN: 0067-2904

## Geochemistry of the kaolinite-rich claystone in Western Iraq

Bashaer Hassoon Abdulmahdi\* Firas Mudhafar Abdulhussein

Department of Geology, College of Science, University of Baghdad, Baghdad

Received: 15/4/2024

Accepted: 21/7/2024

Published: 30/6/2025

### Abstract

It is important to spotlight the non-oil Iraqi wealth used in industry, including the kaolin clays in western Iraq, specifically in Anbar Governorate, where they are found in large quantities suitable for investment. This study focuses on the red kaolin clays found in the Hussainiyat Formation (Lower Jurassic) in the southeast of the Hussainiyat Valley. These clays are important in various industries, including ceramics, cement, and bricks. Geochemical analysis plays an important role in determining the suitability of these clays for industrial use.

Kaolinite was studied in the Northeastern Hussainiyat Area within the Hussainiyat Formation (Lower Jurassic). The presence of kaolinite and illite-smectite was noted, in addition to montmorillonite, quartz, hematite, and goethite. The concentrations of the main oxides in the study area reached  $\text{Al}_2\text{O}_3$  23.35%,  $\text{SiO}_2$  51.33,  $\text{Fe}_2\text{O}_3$  9.05%,  $\text{MgO}$  1.9%,  $\text{CaO}$  1.13%,  $\text{K}_2\text{O}$  1.34%,  $\text{P}_2\text{O}_5$  0.04%, and LOI 10.2%. Aluminium in kaolin clay has a positive relationship with  $\text{Cr}_2\text{O}_3$  and  $\text{TiO}_2$ , a negative relationship with iron, potassium, magnesium, and sodium oxides, and a negative relationship with quartz, which increases with the decrease of these oxides. The deposits were chemically classified into shale and Fe-shale and formed in extensive weathering.

**Keywords:** Red kaolin, Hussainiyat Formation, Western Iraq, Geochemistry, Clay Minerals

### جيوكيمياء الحجر الطيني الغني بالكاولينيت في غرب العراق

بشائر حسون عبد المهدي\* , فراس مظفر عبد الحسين

<sup>1</sup> قسم علم الارض , كلية العلوم , جامعة بغداد , بغداد

### الخلاصة

من المهم تسليط الضوء على الثروات العراقية غير النفطية المستخدمة في الصناعة، ومنها طين الكاولين في غرب العراق، وتحديدًا في محافظة الأنبار، حيث يتواجد بكميات كبيرة صالحة للاستثمار. في هذه الدراسة تمت دراسة وتحليل طين الكاولين الأحمر في تكوين الحسينيات (الجوراسي السفلي) جنوب شرق وادي الحسينيات، وتحليله جيوكيميائياً نظراً لأهميته في الصناعة مثل صناعة السيراميك والأسمت والطوب وغيرها، حيث ان التحليل الجيوكيميائي يعتبر من العناصر الأساسية في تحديد الصناعة.

\* Email [bashaer.abd2308@sc.uobaghdad.edu.iq](mailto:bashaer.abd2308@sc.uobaghdad.edu.iq)

تمت دراسة الكاولينيت في منطقة الحسينيات الشمالية الشرقية ضمن تكوين الحسينيات (العصر الجوراسي السفلي). ولوحظ وجود معادن الكاولينيت والإليت السميكتايت بالإضافة إلى المونتموريلونيت والكوارتز والهيماتيت والجويتيت. بلغت تراكيز الأكاسيد الرئيسية في منطقة الدراسة  $\text{Fe}_2\text{O}_3$  51.33 ،  $\text{SiO}_2$  23.35% ،  $\text{Al}_2\text{O}_3$  23.35% ،  $\text{CaO}$  1.13% ،  $\text{K}_2\text{O}$  1.34% ،  $\text{P}_2\text{O}_5$  0.04% ،  $\text{MgO}$  1.9% ،  $\text{LOI}$  10.2% . ولألومنيوم في طين الكاولين علاقة إيجابية مع أكسيد الكروم وأكسيد التيتانيوم، وعلاقة سلبية مع أكاسيد الحديد واليوتاسيوم والمغنيسيوم والصوديوم، وعلاقة سلبية مع الكوارتز الذي يزداد مع نقصان هذه الأكاسيد. تم تصنيف الرواسب كيميائياً إلى صخر زيتي و صخر زيتي حديدي ، وتشكلت في التجوية واسعة النطاق.

## 1. Introduction

Soil is a unique constituent in the biosphere [1], constituting a complicated gravel, silt, sand, and clay [2]. Clay minerals are abundant by weathering besides (low-temperature hydrothermal alteration) natural products. They are abundant minerals in terrestrial structures, exclusively in the pedosphere [3]. One of the clay minerals is kaolinite, which is formed from feldspar by chemical weathering. The color is white and shade gray. The chemical composition of kaolinite is  $\text{Al}_2\text{Si}_2\text{O}_5(\text{OH})_4$  [4]. There are many formations containing kaolin in the Western Desert region of western Iraq, such as the Jeed Formation (Maastrichtian–Danian) [5], Gaara Formation (Permocarboniferous), Hussainiyat Formation (Lower Jurassic), and Amij Formation (Middle Jurassic) [6]. The area previously investigated by Tobia (2005) [7] who studied the sequence of clastic and carbonate rocks in the Desert of Western Iraq in the Jurassic period, including Hussainiyat, Amij, Muhaiwir, and Najmah formations. Kaolin clay was the most common mineral in mud rocks and metal; X-ray diffraction demonstrated that the crystal's diameters differed in their irregularities. Ali et al. (2022) [8] studied samples from the Hussainiyat Formation that have been analysed by mineralogical and chemical methods, XRD appears that kaolinite was the essential mineral in the clay minerals, alongside a few palygorskite, montmorillonite, and illite. Heavy minerals are present in less than 1%. Tamar-Agha et al. (2016) [9] investigated the contradiction between the depositional environments of the Rutba and Hussainiyat Formations, and stated that the Rutba Formation is more evolution than the Hussainiyat Formation. This study spotlights the geochemistry of red kaolin the Hussainiyat Formation for the industrial uses.

### 1.1 Location and Geological Setting of the Study Area

The study area is approximately 120 km north of Rutba City, near the Wadi Horan and Wadi Al-Hussainiyat junction. Figure 1 shows the location of the area under study.

Easting Northing

104537 3674991

Iraq is located on the Arabian Plate in the northeastern part [10] of the Stable Shelf [11]. The area belongs to the Inner Platform region [12], which does not exhibit the effects of Alpine compression or significant Permo-Triassic rifting. The Inner Platform is subdivided into two distinct subzones based on their morphology and physiographic characteristics. The Southern Desert Subzone to the southeast and the Western Desert Subzone to the northwest [13]. Oligocene sediments are absent over most of the Rutba subzone [14].

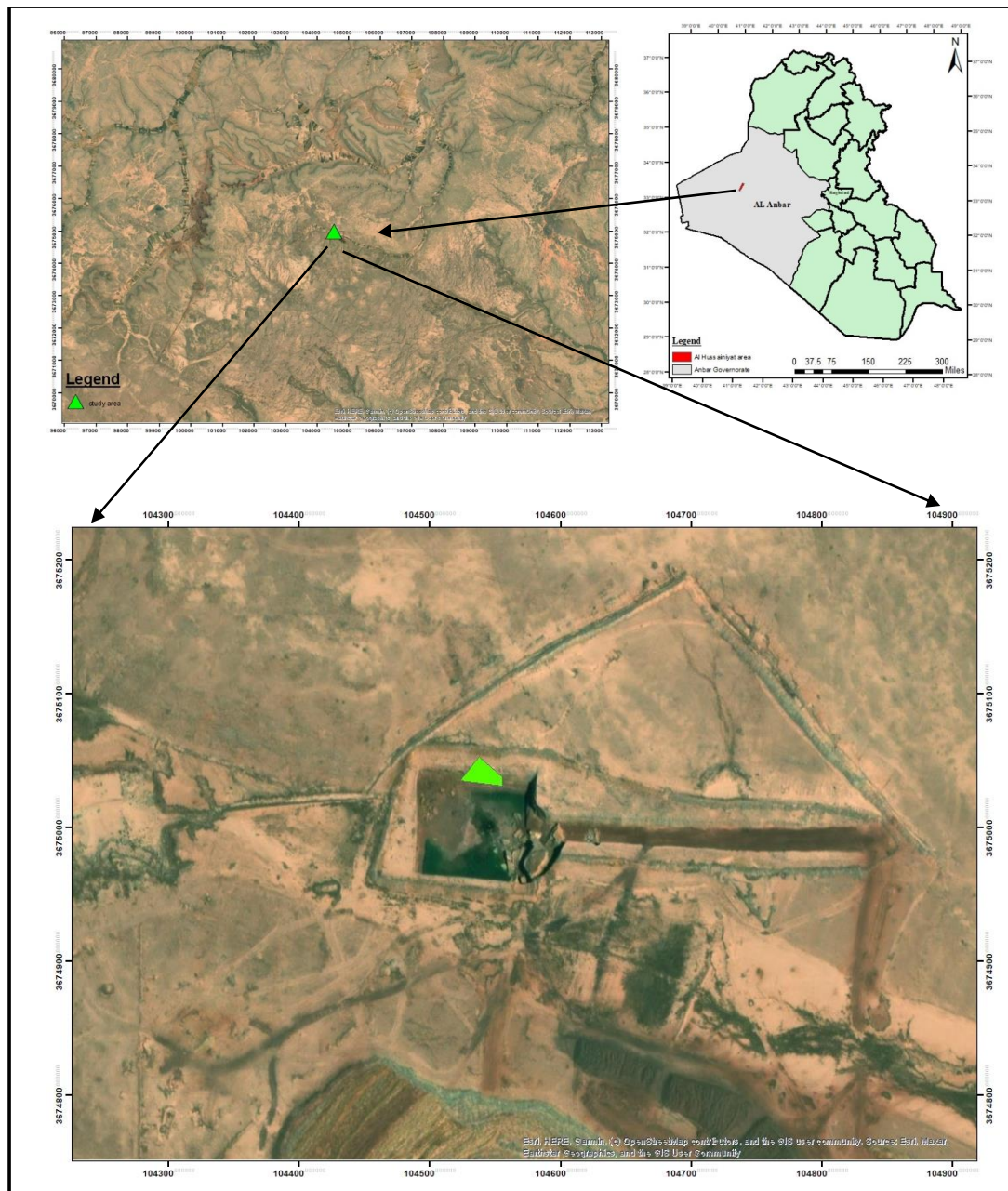


**Figure 1:** Kaolin clay in Hussainiyat Formation in the northern east of Wadi Al Hussainiyat.

The general slope of the study area is 11 m per 1 km toward the southeast [15]. Quaternary sediments cover the area and underlie the exposures of the Ubaid and Hussainiyat Formations [16]. The Hussainiyat Formation, which belongs to the Lower Jurassic, is situated stratigraphically between two other Jurassic formations within the study area. The Amij Formation (Middle Jurassic) overlies the Hussainiyat Formation, and the Ubaid Formation (Lower Jurassic) underlies the Hussainiyat Formation [13]. The lower contact with the Ubaid Formation is observed as an unconformable erosional surface displaying significant undulations and subsidence. In contrast, the upper contact with the Amij Formation is conformable without interruption [15]. Figure 2 shows the stratigraphic column of the Hussainiyat Formation, which is divided into the following units:

- **Lower unit (Hussainiyat clastic)**

This unit exhibits a variable thickness, reaching a maximum of 54 m in the area 2 km south of the Hussainiyat dome. It comprises a sequence of claystone and sandstone, with iron ore lenses in the southeastern and central parts of the unit. The northeastern part of the unit shows an interbedding of claystone, sandstone, and kaolin. The sandstones exhibit a range of colors, including white, yellow, and reddish-brown, and are mottled with dark brown spots. Grain sizes vary from coarse to very coarse. The upper part of the sandstone is finer-grained, ferruginous, and sometimes quarzitic, with cross-bedding. The claystone exhibits a spectrum of colors from red and reddish-brown through violet to pink. Iron ore deposition is principally concentrated inside the claystone sequences, occurring as horizontal and lenticular configurations [15].

- **Upper unit (Hussainiyat Marker):**

This unit has varying thicknesses, rising from the study area southeast to northeastern regions. The thickness varies from 7 to 8 m in the middle to up to 15 m in the northeast section. Reddish-brown sandy shelly limestone with sporadic lenses of quarzitic sandstone makes up this unit, a notable marker horizon.

A varied thickness is also seen in the upper carbonate member of the Hussainiyat Formation, which increases from the southeast (40 m) to the northwest (50 m) of the studied region. A maximum thickness of 56 m was reported 3.5 km south of the Muhaiwir castle. This upper carbonate member comprises dolostone, dolomitic limestone, and fossiliferous limestone, with a gray to brownish-gray in color. The rocks are highly fractured, and secondary calcite crystals fill the cavities [15].

- **The upper carbonate**

The upper carbonate member of the Hussainiyat Formation also has a variable thickness, increasing from the southeastern (40 m) to the northwestern (50 m) part of the study area, with a maximum thickness of 56 m observed at 3.5 km south of the Muhaiwir castle. The dominant carbonate rocks comprising this type of upper interval include dolomitic limestone, fossiliferous limestone, and dolostone. They exhibit gray to light brownish-gray color. The rocks exhibit significant weathering and fracturing, with crystalline fill made of secondary calcite filling the cracks and fissures [13].

In contrast, the Bajocian (Middle Jurassic) age [17] has been suggested for the formation based on the bivalve species *Anisocardia* [18]. The lower clastic age unit of the Hussainiyat Formation has been determined as Hettangian-Pliensbachian (Liassic) based on the stratigraphic evidence and palynomorph assemblages [15, 19].

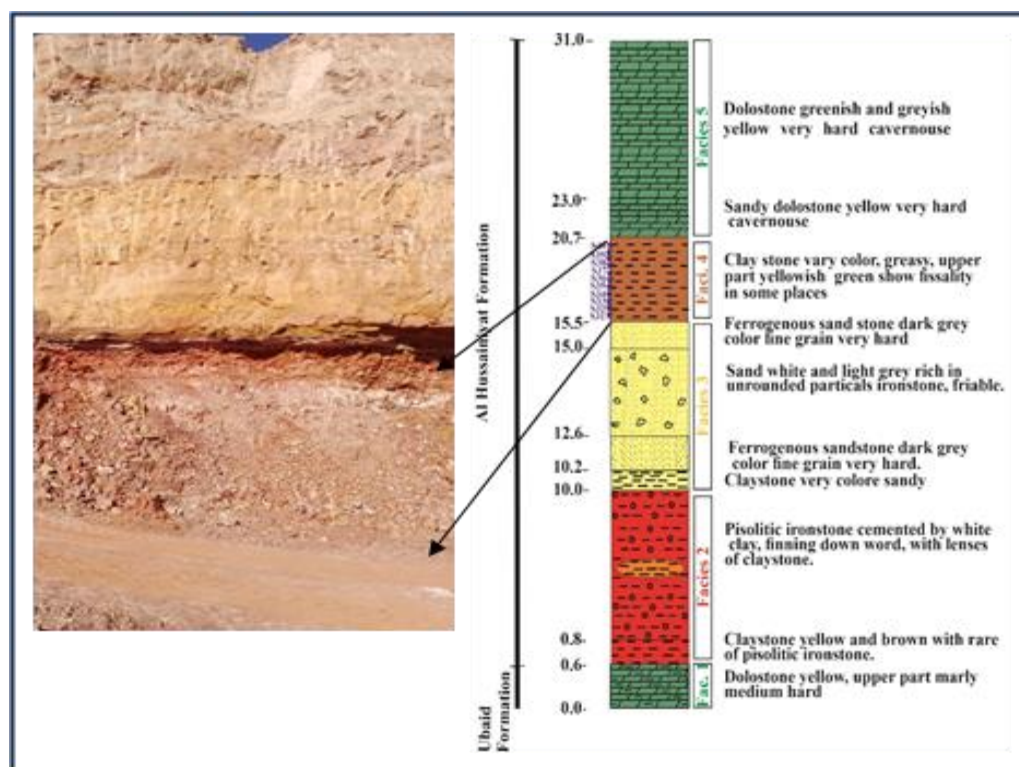


**Figure 2:** Columnar section of Al Hussainiyat Formation

## 2. Materials and methods

The sampling was done from a stratigraphy section of the Hussainiyat Formation with the help of excavators since the area is invested (iron quarries). Twelve samples were collected from the kaolin clay layer.

### 2.1. X-Ray Diffraction

It uses powder samples for X-ray diffraction examination. The powders were placed within aluminium sample holders after a fine crushing of the samples. The samples were subsequently examined using an X-ray diffractometer in the Al Khora laboratory, Baghdad. The following circumstances applied to the diffractometer's operation: Cu K-alpha radiation was produced using a 1.0 degree divergence slit, a 0.15 mm reception slit, and a 1.0-degree scatter slit at 40 kV and 30 mA. Using a continuous scan mode with a step size of 0.05 degrees and a scan speed of 5 degrees per minute, counts were acquired for 0.6 seconds per step over a 2-theta scan range of 5.6-80 degrees. Twelve samples from the kaolin layer in the Hussainiyat Formation were used.

### 2.2. Scanning electron microscope SEM

The outer surface of the samples was dried at 80 C and examined using a scanning electron microscope ( JEOL model JSM5410 LV) in Al-Khora Laboratory in Baghdad. Before the analysis, the sample was coated with a thin layer of gold to increase conductivity and reduce charge under the electron beam. An accelerating voltage of 15 kV was used under high vacuum (10-5 Pa). Four samples were examined by this technique.

### 2.3. Chemical Analysis

The samples were analyzed for major oxide in ALS laboratories in Spain/Seville and are within the specifications in Table 1 Below. Selected 12 samples to do the chemical analysis.

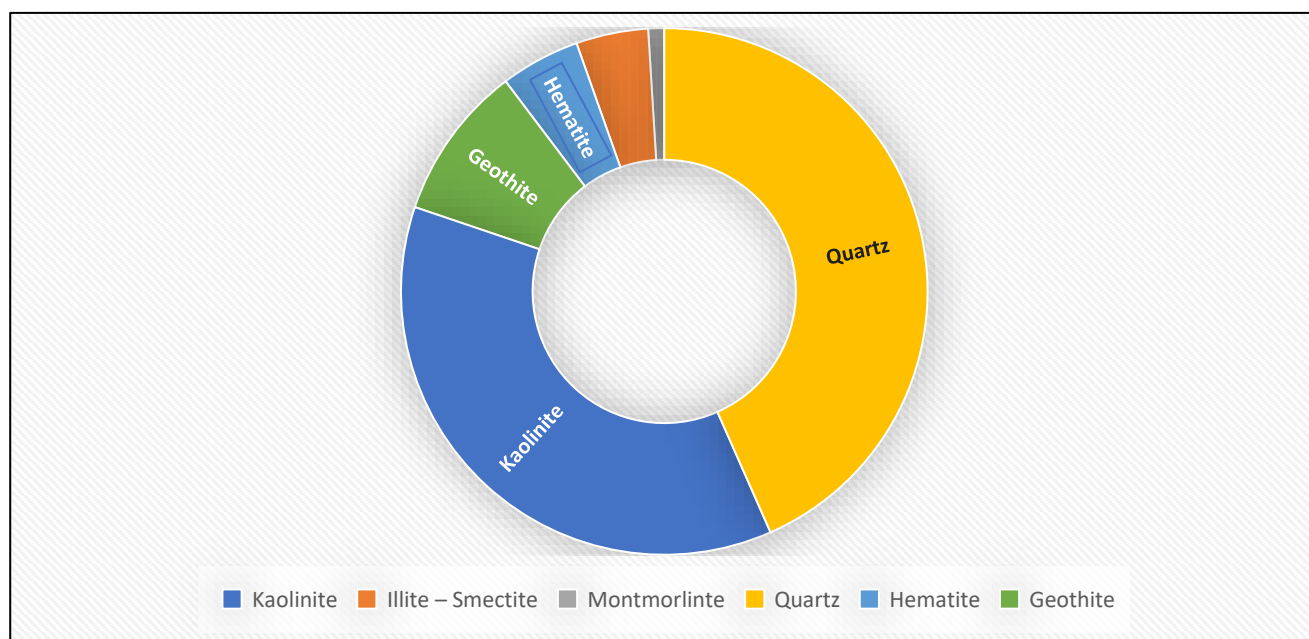


**Table 1:** shows the analytical procedures

Analytical Procedures		
ALS Code	Description	Instrument
ME-4ACD81	Base metals by 4-acid dig	ICP-AES
ME-XRF26	Whole Rock by Fusion/XRF	XRF
OA-GRA05x	LOI at 1000C for XRF	WST-SEQ

### Results and Discussion

The results of XRD showed a high quantity of quartz in the rocks, reaching an average percentage of 44.3%. As for kaolinite, it is present at a rate of 37.6%. Goethite, hematite, and illite-smectite also occur at a rate of 9.7, 4.9, and 4.5, respectively, and appear as 1% of montmorillonite. Figure 2 is a detailed explanation of the XRD results of clay minerals. The detailed constituents of mineralogy is presented in Figure 3.

**Figure 3:** Distribution of clay minerals in study samples by XRD technique

In a Scanning electron microscope, kaolinite appears as a stack of vermicular or smaller, less clear crystals [20], as shown in Figure 4

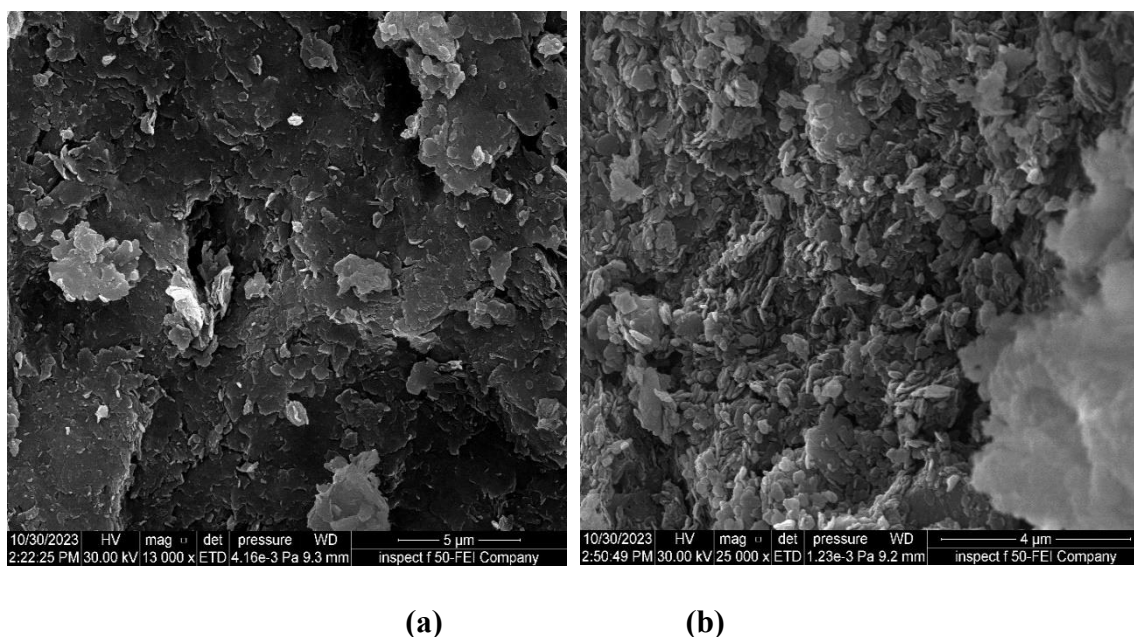


**Figure 4:** Kaolin clay under the Scanning Electron Microscope (SEM) (a) and (b)

SiO<sub>2</sub> ranged between 41.68% and 67.29% in kaolin clay, averaging 52.8% less than PAAS (10%) and less than UCC (12.12%). Al<sub>2</sub>O<sub>3</sub> ranged between (18.16% - 33.94%), and the average is 24.1% more than PAAS at (5.2%) and more than UCC at (9.4%). The concentration of Fe<sub>2</sub>O<sub>3</sub> ranges between 1.35% and 18.22% and the average is 8.8%, represented as goethite and hematite more than PAAS (2.3%) and more than UCC (4.4%). TiO<sub>2</sub> in the kaolin clays of the Al Hussainiyat Formation ranges between 1.21% and 2.08%. The average is 1.6% more than PAAS (0.6%) and more than UCC (1.1%). K<sub>2</sub>O (0.04% - 3.66%), and the average (1.3%) less than PAAS at (2.4%) and UCC at (2.1%). CaO ranged between (0.24% - 0.68%), and the average is 0.4% less than PAAS (0.9%) and less than UCC (3.7%). MgO ranged between (0.35% - 2.67%), and the average is (1.4%) less than PAAS (0.8%) and less than UCC (0.8%). P<sub>2</sub>O<sub>5</sub> ranges between 0.02% and 0.07% and averages 0.04% less than PAAS (0.1%) and less than UCC (0.1%). Sodium oxide (Na<sub>2</sub>O) is ranged from 0.07% to 0.18%. The average is 0.13% less than PAAS (1.1%) and less than UCC (3.3%). Chromium (III) oxide (Cr<sub>2</sub>O<sub>3</sub>) ranges between 0.01% and 0.05% and an average of 0.02%. Strontium oxide (SrO) ranges between (<0.01% - 0.02%), and an average of 0.012%, Manganese (II) oxide (MnO) ranges between (<0.01% - 0.03%), and the average of 0.02, And Barium oxide (BaO) ranged in <0.01. The low percentages of calcium oxide and magnesium oxide indicate the low rate of carbonates in kaolin clay. The concentrations of LOI ranged between (7.05% - 12.75%), and the average is 9.4%, represented by H<sub>2</sub>O in the crystal of clay minerals, more than PAAS in (3.4%). Table 2 shows the details of the chemical composition of Oxides for 12 samples. Our studied kaolin-rich characteristics by SiO<sub>2</sub> lower than PAAS and UCC indicate our claystone was affected by more chemical weathering and is highly sorted. Al<sub>2</sub>O<sub>3</sub>, Fe<sub>2</sub>O<sub>3</sub>, and TiO<sub>2</sub> are the oxides displaced enrichment in our studied claystone. These immobile oxides indicate that the source rock is affected by intensive chemical weathering. CaO, MgO, and K<sub>2</sub>O show demolishing because these mobile elements are highly affected and dissolve by chemical weathering [21].

**Table 2:** The concentration of chemical composition of kaolin

Sample	SiO <sub>2</sub>	Al <sub>2</sub> O <sub>3</sub>	Fe <sub>2</sub> O <sub>3</sub>	MgO	CaO	TiO <sub>2</sub>	Na <sub>2</sub> O	K <sub>2</sub> O	P <sub>2</sub> O <sub>5</sub>	Cr <sub>2</sub> O <sub>3</sub>	MnO	SrO	LOI
S10	41.68	33.94	8.97	0.52	0.28	1.92	0.09	0.09	0.07	0.03	<0.01	<0.01	12.42
S11	46.39	36.34	1.35	0.57	0.31	2.08	0.1	0.1	0.04	0.05	<0.01	0.01	12.75
S12	53.66	29.52	2.47	0.5	0.31	1.91	0.08	0.07	0.05	0.03	<0.01	<0.01	10.6
S13	67.29	21.1	1.48	0.35	0.24	1.21	0.07	0.04	0.02	0.02	<0.01	<0.01	7.78
S31	54.07	21.76	10.9	0.94	0.3	1.94	0.1	0.76	0.05	0.02	0.01	0.01	8.72
S32	57.72	24.06	4.18	0.98	0.31	2.06	0.11	0.83	0.04	0.02	0.01	0.01	9.02
S33	62.46	18.16	7.91	1.42	0.38	1.41	0.1	1.38	0.04	0.01	0.01	0.01	7.05
S34	50.36	20.5	12.6	2.54	0.66	1.41	0.17	2.93	0.05	0.01	0.02	0.01	8.82
S36	48.44	22.08	14.34	2.03	0.52	1.54	0.16	2.05	0.05	0.02	0.02	0.02	9.04
S37	48.57	20.16	18.22	1.91	0.65	1.44	0.17	1.48	0.04	0.02	0.03	0.01	9
S38	50.84	21.05	11.7	2.48	0.68	1.42	0.18	2.64	0.05	0.01	0.01	0.02	9.45
S39	52.39	20.21	11.39	2.67	0.61	1.4	0.17	3.66	0.02	0.01	<0.01	0.01	8.22
average	52.8	24.1	8.8	1.4	0.4	1.6	0.13	1.3	0.04	0.02	0.02	0.012	9.4
Min.	41.68	18.16	1.35	0.35	0.24	1.21	0.07	0.04	0.02	0.01	0.01	0.01	7.05
Max.	67.29	36.34	18.22	2.67	0.68	2.08	0.18	3.66	0.07	0.05	0.03	0.02	12.75
PAAS	62.8	18.9	6.5	2.2	1.3	1	1.2	3.7	0.16	-	-	-	6
UCC	64.92	14.63	4.42	2.24	4.12	0.52	3.46	3.45	0.15	-	-	-	-

The concentrations compared with Upper Continental Crust (UCC) [22], and Post-Archean Australian Shale (PAAS) [23].

The correlation coefficient between Cr<sub>2</sub>O<sub>3</sub> and TiO<sub>2</sub> is very high and positive, which means it is connected with aluminium by adsorbed or on the side of the structure of kaolin.

The positive relationship between Cr<sub>2</sub>O<sub>3</sub> and Al<sub>2</sub>O<sub>3</sub> is because Cr can replace Al. Titanium comes in aluminium (detrital), and part of B<sub>2</sub>O<sub>3</sub> is transported with aluminium. Fe<sub>2</sub>O<sub>3</sub>, K<sub>2</sub>O, MgO, and Na<sub>2</sub>O have a negative relationship with Al<sub>2</sub>O<sub>3</sub>. When Al<sub>2</sub>O<sub>3</sub> increases, they decrease, knowing that K<sub>2</sub>O is an essential oxide of illite–smectite, and this oxide decreases the kaolinite amount in the rock. CaO, MgO is 0.9, which means there is dolomite, but there is very little quantity in clay minerals. Al<sub>2</sub>O<sub>3</sub> and SiO<sub>2</sub> have a negative relationship, meaning the quartz is high in quantity [7]. Table 2 shows the correlation coefficient of the content of kaolin.

**Table 3:** The correlation Coefficient of the chemical composition of kaolin clay in the study area

	SiO <sub>2</sub>	Al <sub>2</sub> O <sub>3</sub>	Fe <sub>2</sub> O <sub>3</sub>	MgO	CaO	TiO <sub>2</sub>	Na <sub>2</sub> O	K <sub>2</sub> O	P <sub>2</sub> O <sub>5</sub>	Cr <sub>2</sub> O <sub>3</sub>	LOI
SiO <sub>2</sub>	1										
Al <sub>2</sub> O <sub>3</sub>	-0.539	1									
Fe <sub>2</sub> O <sub>3</sub>	-0.416	-0.517	1								
MgO	-0.201	-0.617	0.750	1							
CaO	-0.310	-0.516	0.777	0.949	1						
TiO <sub>2</sub>	-0.390	0.744	-0.403	-0.564	-0.560	1					
Na <sub>2</sub> O	-0.381	-0.476	0.800	0.953	0.971	-0.449	1				
K <sub>2</sub> O	-0.125	-0.618	0.654	0.978	0.879	-0.560	0.889	1			
P <sub>2</sub> O <sub>5</sub>	-0.645	0.425	0.220	-0.123	-0.054	0.466	-0.032	-0.214	1		
Cr <sub>2</sub> O <sub>3</sub>	-0.382	0.906	-0.530	-0.692	-0.567	0.701	-0.521	-0.719	0.209	1	
LOI	-0.737	0.954	-0.279	-0.417	-0.275	0.688	-0.231	-0.456	0.550	0.832	1



The chemical classification according to the diagram of Herron (1988) indicates that the kaolin in the Hussainiyat Formation fluctuates between shale and Fe-shale. Figure 5 The chemical classification according to the diagram of Herron (1988)

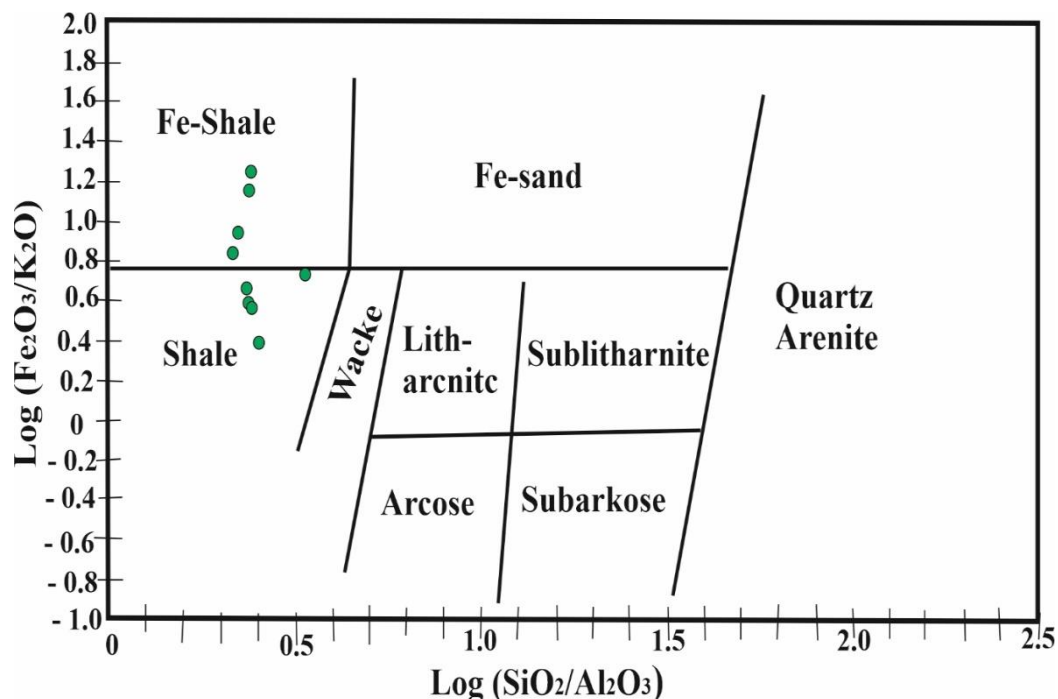


**Figure 5:** The chemical classification according to the diagram of Herron (1988) [24]

The intensity of the alteration of feldspar to clay by weathering can be determined through (chemical index alteration CIA) [25]. This process has been done by measuring the loss of alkaline, and alkaline earth elements such as sodium, calcium, and potassium [26]. And calculated by :

$$CIA = [Al_2O_3 / (Al_2O_3 + CaO + Na_2O_3 + K_2O)] * 100 \quad \dots\dots\dots(1)$$

The CIA classification is considered [27];[28]:

50 – 60 %:- low weathering

60 – 80%:- an intermediate weathering

80 – 100%:- extensive weathering

According to the CIA rate for the kaolin clays of the Hussainiyat Formation Table 3, it formed in extensive weathering. When plotting the values of  $Al_2O_3$  with the CIA [29]; [30], it was noticed that kaolin clay was formed during extensive weathering (Figure 6).

**Table 4:** Chemical index alteration of kaolin clay of Al Hussainiyat Formation

Samples	S10	S11	S12	S13	S31	S32	S33	S34	S36	S37	S38	S39	Avg.
CIA	98.66	98.62	98.47	98.37	94.94	95.06	90.71	84.50	89.00	89.76	85.74	81.99	92.15

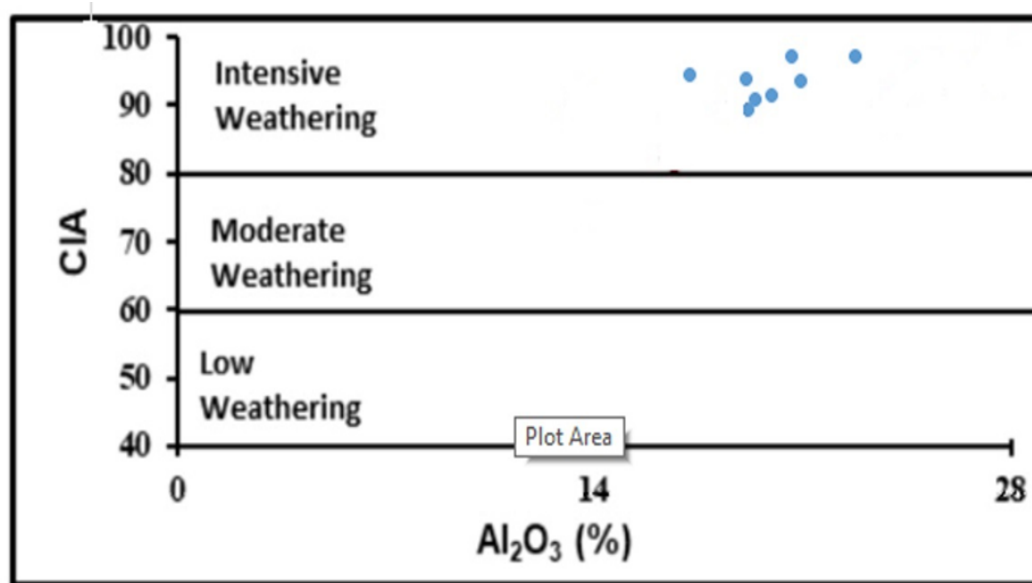


**Figure 6:** shows the weathering intensity for kaolin clay in the Al Hussainiyat Formation.

### Conclusions

The kaolin in the Hussainiyat Formation belongs to the Lower Jurassic age. It was noted that the percentage of quartz in it reached 44.3%, and the rate of kaolin reached 37.6, in addition to the presence of illite-smectite at a rate of 4.5%, goethite at 9.7%, and hematite at 4.9%, and there was a 1% of montmorillonite in the study area.

In a Scanning electron microscope, kaolinite appears as a stack of vermicular or smaller, less clear crystals. The distinctive characteristic of Hussainiyat kaolin is its red color due to the presence of iron oxides, the percentage of which in chemical analyses reaches 9%, which is 2.55% higher than Post-Archean Australian Shale (PAAS) and 4.63% higher than Upper Continental Crust (UCC) on average. Kaolin-rich characteristics by SiO<sub>2</sub> lower than PAAS and UCC indicate our claystone was affected by more chemical weathering and is highly sorted. Al<sub>2</sub>O<sub>3</sub>, Fe<sub>2</sub>O<sub>3</sub>, and TiO<sub>2</sub> are the oxides displaced enrichment in our studied claystone. These immobile oxides indicate that the source rock is affected by intensive chemical weathering. CaO, MgO, and K<sub>2</sub>O show demolishing because these mobile elements are highly affected and dissolve by chemical weathering. Correction coefficient showed that Cr<sub>2</sub>O<sub>3</sub> and TiO<sub>2</sub> have a positive relationship with aluminium because chromium can replace aluminium, and noticed a negative relationship for aluminium with iron, potassium, magnesium, and sodium oxides, meaning that when aluminium increases, this group decreases. As for silica and aluminium, they have a negative relationship, meaning that quartz is present in large quantities. When observing the chemical classification of Herron (1988), kaolin clays fall within the shale to Fe - shale. The kaolin clay in the Hussainiyat Formation was formed by extensive weathering.

### Acknowledgements

Thanks to Dr. Ibrahim Qasim Mohammed, Al-Maarif University College, for his assistance during fieldwork and all laboratory analysis and fieldwork, and Dr. Jalal Naser Jabur, Department of Chemistry at the University of Baghdad, College of Science, for assistance. And thanks to Mr. Wisam Meiagal, a Geologist, for assessing the fieldwork.

## References

- [1] F. Abdulhussein And H. Mazin, "Distribution And Evaluation Of Lead And Cadmium In Some Soils Surrounding East Baghdad Oil Field," Iraqi Journal Of Science, Vol. 64, Pp. 4002-4017, 08/30 2023.
- [2] F. Abdulhussein And H. Mazin, "Evaluation Of Vanadium Contamination In Some Soils Of The East Baghdad Oil Field," Iraqi Journal Of Science, Vol. 64, Pp. 2959-2972, 06/30 2023.
- [3] L. Zhang, G. M. Gadd, And Z. Li, "Chapter Four - Microbial Biomodification Of Clay Minerals," In Advances In Applied Microbiology. Vol. 114, G. M. Gadd And S. Sariaslani, Eds., Ed: Academic Press, 2021, Pp. 111-139.
- [4] N. Av, S. D. Raj, And M. Soman, A Review On Microstructural, Mechanical, And Durability Characteristics Of Raw Kaolin Clay-Based Geopolymers, 2024.
- [5] I. Q. Mohammed, S. Farouk, A. Mousa, And F. A. Lawa, "Lithofacies Types, Mineralogical Assemblages And Depositional Model Of The Maastrichtian–Danian Successions In The Western Desert Of Iraq And Eastern Jordan," Journal Of African Earth Sciences, Vol. 186, P. 104397, 2022/02/01/ 2022.
- [6] M. Y. Tamar-Agha, M. A. Mahdi, And A. A. A. Ibrahim, "The Kaolin Clay Deposits In The Western Desert Of Iraq: An Overview," 2019.
- [7] F. Tobia, "Mineralogy And Geochemistry Of The Clastics Of Jurassic System In Iraqi Western Desert," Unpub. Ph. D. Thesis, 2005.
- [8] R. Ali, H. Jassim, Al, And Fe, "Mineralogy, Geochemistry, And The Origin Of Lower Clastic Unit In Hussainiyat Formation (Early Jurassic) Western Desert Of Iraq," Vol. Vol.18, No.1, Pp. 1-19, 01/01 2022.
- [9] M. Tamar-Agha, A. Al-Zubaidi, And S. Al-Janabi, "A Comparative Study Between The Depositional Environment And Provenance Of The Hussainiyat (Lower Jurassic) And The Rutbah (Upper Cretaceous) Formations, Western Desert Of Iraq," Arabian Journal Of Geosciences, Vol. 9, 05/01 2016.
- [10] A. I. Al-Juboury, N. T. Al-Tae, And Z. A. Malak, "Paleoenvironmental Conditions During Deposition Of Kolosh And Gercus Formations In Northern Iraq As Deduced From Clay Mineral Distributions," Iraqi Journal Of Science, Vol. 62, Pp. 4791-4801, 12/30 2021.
- [11] A. Mousa, S. Al-Dulaimi, And I. Mohammed, Q., "Microfacies Analysis Of The Late Maastrichtian-Danian Phosphatic Succession In The H3-Trebeel District, Western Desert Of Iraq " Iraqi Journal Of Science, Vol. 26, Pp. 1188-1203, 04/30 2021.
- [12] M. Y. Tamar-Agha And S. H. Al-Hazaa, "Lower Permian Fluvial Sediments, Ga'ara Depression, Western Iraq: Depositional Environment And Hydrocarbon Potential," Iraqi Journal Of Science, Vol. 64, Pp. 2913-2933, 06/30 2023.
- [13] M. A. A. Mahdi, " Minerological And Chemical Composition And Depositional Environment Of Kaolinitic Claystones Of Hussainiyat Formation In North Eastren Part Of Hussainiyat Valley, Western Desert, Iraq," Iraqi Bulletin Of Geology And Mining,, Vol. 2, Pp. 9 – 22., 2006.
- [14] F. Abdulhussein And S. Hussein, "Hydrochemical And Isotopic Study Of Water Resources In Khan Al-Baghdadi Area, Al- Anbar Province/West Of Iraq," Iraqi Journal Of Science, Vol. 62, Pp. 204-217, 01/30 2021.
- [15] V. Sissakian And B. Mohammed, "Stratigraphy Of The Iraqi Western Desert," Iraqi Bulletin Of Geology And Mining, Vol. Special Issue No.1, Pp. 51-124, 01/01 2007.
- [16] N. T. Altaee And Z. A. Malak, "Facies Analysis And Depositional Environments Of The Ubaid Formation, Western Iraq," Iraqi Journal Of Science, Vol. 62, Pp. 2580-2588, 08/31 2021.
- [17] K. M. Hassan, "Jurassic Mollusco From Western Desert, Iraq," M.Sc.Thesis, University Of Hall, U.K, P. 210p, 1984.
- [18] B. S. Al-Jibouri, "Palynostratigraphy Of The Lower Clastic Unit Of Hussainiyat Formation (Early Jurassic), Western Desert, Iraq,," Iraqi Bulletin Of Geology And Mining Vol. 6, Pp. 21-29, 2010.
- [19] T. Buday And J. Hak, "The Geological Survey Of The Western Part Of The Western Desert. No.1000,," The State Company Of Geological Survey And Mining, Iraq, 1980.
- [20] M. J. Wilson, A Handbook Of Determinative Methods In Clay Mineralogy / Edited By M.J. Wilson. Glasgow : New York, 1987.

- [21] S. M. McLennan, S. Hemming, D. K. McDaniel, G. N. Hanson, M. J. Johnsson, And A. Basu, "Geochemical Approaches To Sedimentation, Provenance, And Tectonics," In Processes Controlling The Composition Of Clastic Sediments. Vol. 284, Ed: Geological Society Of America, 1993, P. 0.
- [22] S. M. McLennan, "Relationships Between The Trace Element Composition Of Sedimentary Rocks And Upper Continental Crust," *Geochemistry, Geophysics, Geosystems*, Vol. 2, 2001.
- [23] S. R. Taylor And S. M. McLennan, "The Continental Crust: Its Composition And Evolution," *J Geol*, Vol. 94, Pp. 57-72, 01/01 1985.
- [24] M. Herron, "Geochemical Classification Of Terrigenous Sands And Shales From Core Or Log Data," *Journal Of Sedimentary Research - J Sediment Res*, Vol. 58, 01/01 1988.
- [25] J. Shao, S. Yang, And C. Li, "Chemical Indices (Cia And Wip) As Proxies For Integrated Chemical Weathering In China: Inferences From Analysis Of Fluvial Sediments," *Sedimentary Geology*, Vol. 265-266, Pp. 110-120, 2012/07/15/ 2012.
- [26] K. M. Kee, E. Sathiamurthy, K. Sultan, And Z. Liu, "Geochemical Characterization Of Clay Minerals In Surface Sediments Of Three Major Rivers Along The East Coast Of Peninsular Malaysia," *Bulletin Of The Geological Society Of Malaysia*, Vol. 61, Pp. 23-28, 12/01 2015.
- [27] M. Singh, M. Sharma, And H. Tobschall, "Weathering Of The Ganga Alluvial Plain, Northern India: Implications From Fluvial Geochemistry Of The Gomati River," *Applied Geochemistry*, Vol. 20, Pp. 1-21, 01/31 2005.
- [28] A. Gupta, *Large Rivers: Geomorphology And Management*: Wiley, 2022.
- [29] H. W. Nesbitt And G. Young, "Early Proterozoic Climates And Plate Motions Inferred From Major Element Chemistry Of Lutites," *Nature*, Vol. 299, 10/21 1982.
- [30] R. Obasi, H. Madukwe, And P. Nnabo, "Geochemistry, Weathering Intensity And Paleo- Climatic Conditions Of Soils Around Dumpsites From Ibadan, Oyo State, Nigeria," 06/10 2020.